Experimental Equilibrium Structures: Application of Molecular Dynamics Simulations to Vibrational Corrections for Gas Electron Diffraction

Derek A. Wann,[†] Alexander V. Zakharov,[‡] Anthony M. Reilly,[†] Philip D. McCaffrey,[†] and David W. H. Rankin*,[†]

School of Chemistry, University of Edinburgh, West Mains Road, Edinburgh, U.K. EH9 3JJ, and Department of Physics, Ivanovo State University of Chemistry and Technology, Engelsa 7, Ivanovo 153000, Russian Federation

Received: May 5, 2009; Revised Manuscript Received: July 2, 2009

A general method is described that allows experimental equilibrium structures to be determined from gas electron diffraction (GED) data. Distance corrections, starting values for amplitudes of vibration and anharmonic "Morse" constants (all required for a GED refinement) have been extracted from molecular dynamics (MD) simulations. For this purpose MD methods have significant advantages over traditional force-field methods, as they can more easily be performed for large molecules, and, as they do not rely on extrapolation from equilibrium geometries, they are highly suitable for molecules with large-amplitude and anharmonic modes of vibration. For the test case $Si_8O_{12}Me_8$, where the methyl groups rotate and large deformations of the Si_8O_{12} cage are observed, the MD simulations produced results markedly superior to those obtained using force-field methods. The experimental equilibrium structure of $Si_8O_{12}H_8$ has also been determined, demonstrating the use of empirical potentials rather than DFT methods when such potentials exist. We highlight the one major deficiency associated with classical MD—the absence of quantum effects—which causes some light-atom bonded-pair amplitudes of vibration to be significantly underestimated. However, using $C_3N_3Cl_3$ and $C_3N_3H_3$ as examples, we show that path-integral MD simulations can overcome these problems. The distance corrections and amplitudes of vibration obtained for $C_3N_3Cl_3$ are almost identical to those obtained from force-field methods, as we would expect for such a rigid molecule. In the case of $C_3N_3H_3$, for which an accurate experimental structure exists, the use of path-integral methods more than doubles the C−H amplitude of vibration.

Introduction

Structures of molecules in the gas phase are of particular value to chemists and others because the molecules are free from intermolecular forces that can, and often do, distort their geometries. The experimental structures of isolated molecules can then be compared directly with those given by theory, assuming vibrational motion in the gas phase can be accounted for. With the use of computational techniques in all areas of chemistry expanding rapidly, the accuracy of computed structures is vitally important. Molecular mechanics (MM) modeling programs are used extensively in materials and biological chemistry and it is noteworthy that the parametrization of force fields used in MM is largely performed using experimental gas-phase data. Determining experimental gas-phase structures with highly accurate treatments of vibrational effects is therefore an extremely important goal.

Microwave spectroscopy can provide very accurate geometrical and vibrational information for some very small molecules, leading to precise equilibrium structures, using methods such as MORBID.[1] The applicability of microwave spectroscopy is hampered, however, by the requirement of a permanent dipole moment. For all but the smallest molecules it is also necessary to study many isotopomers to determine complete structures.

Gas electron diffraction (GED) is more widely applicable than microwave spectroscopy, with volatility, vaporization rate and thermal stability the major considerations for study feasibility. Assuming that none of these is a barrier to the collection of good quality diffraction data, the last remaining hurdle is the accurate treatment of vibrations. As electron-diffraction experiments yield time-averaged structures, in which interatomic distances may have been affected by vibrations,[2] it is common practice to compute corrections to apply to the distances. This allows a more accurate comparison between theoretical and experimental structures to be made, as well as dealing with possible geometric inconsistencies.

Distance corrections have traditionally been computed using harmonic force fields (experimental or theoretical), although this has sometimes led to the introduction of errors in the corrections that are larger than the corrections themselves. Early programs[3] modeled atomic motion using a rectilinear approach and later a more realistic description was achieved using first-order curvilinear distance corrections.[4]

With the increasing availability of better computational resources, the calculation of cubic anharmonic force fields became feasible for many molecules.[5] While this went some way toward overcoming the deficiencies in the treatment of anharmonic motion by including higher-order terms than are included in harmonic force fields, the method still relies on extrapolation of information from the equilibrium position and so continues to describe large-amplitude motions poorly. This is particularly true when curvilinear motions of atoms include

* To whom correspondence should be addressed. E-mail: d.w.h.rankin@ed.ac.uk.
[†] University of Edinburgh.
[‡] Ivanovo State University of Chemistry and Technology.

10.1021/jp904185g CCC: $40.75
Published on Web 07/31/2009

components that are circular (or arcs of circles), as these are not fitted well even by high-order polynomials.

Recently, the EXPRESS method[6] was developed as a new approach to solving this old problem. EXPRESS explores a much more extensive region of the potential-energy surface (PES) by performing calculations that explicitly probe the energy along internal coordinates relating to each vibrational mode of the molecule. Data are extracted for each unique distance in the molecule and corrections are determined that can be applied to the vibrationally averaged distances to yield experimental equilibrium distances. This method was tested for sodium chloride,[6] which is present as both monomer and dimer in the gas phase, and proved very useful, with good agreement with theory achieved. However, the EXPRESS method is very labor intensive and computationally demanding. Moreover, for a molecule with *N* vibrational modes, it only explores *N* one-dimensional slices of the PES, rather than the whole *N*-dimensional surface.

A less involved method of exploring structures on the potential-energy surfaces of molecules is to use molecular dynamics (MD) simulations. MD uses even more computer resources but may be less labor intensive. A major advantage of MD for this purpose is that it can be applied to molecules of any size, as well as being suitable for determining equilibrium structures in the solid state.[7] We have used the MD method to determine the gas-phase structures of two polyhedral oligomeric silsesquioxanes, $Si_8O_{12}H_8$ and $Si_8O_{12}Me_8$.[8] The focus of that initial paper was the chemistry of these molecules and discussion of the underlying MD method was limited to the essentials. The silsesquioxane molecules are ideal candidates for study by MD because of their relatively large amplitudes of vibration, and their extreme anharmonicity. Here we expand on this work, giving details of a number of different computational methods that can be used to estimate distance corrections and amplitudes of vibration. While simulations using density functional theory (DFT) are still time-consuming, they yield accurate estimates of the vibrational corrections required to determine gas-phase equilibrium structures. Molecular dynamics simulations have also been performed for $Si_8O_{12}H_8$ and $Si_8O_{12}Me_8$ using empirical potentials (EP). EP-MD simulations are substantially faster than DFT-MD ones, but often generic parameter sets must be used, limiting the accuracy of such methods.

Standard MD simulations, whether DFT or EP, use classical equations of motion to model the dynamic behavior of the system. This neglects potential quantum effects that can lead to underestimation of distance corrections and amplitudes of vibration. Path-integral (PI) MD simulations[9,10] replace the classical system with *P* replicas tethered by harmonic forces. This method of simulation allows correct modeling of static quantities of the system, including amplitudes of vibration and vibrational corrections, by incorporating more and more of the quantum behavior as *P* increases. However, as *P* replicas of the system are computed, the calculation takes *P* times as long as a classical simulation, greatly increasing the computational cost, which is especially serious if DFT is being employed. To illustrate how this method can overcome the deficiencies of the classical DFT-MD simulations, a series of simulations have been performed on 1,3,5-triazine ($C_3N_3H_3$). The experimental structure of $C_3N_3H_3$ has previously been determined with extreme precision and accuracy using a combination of data from GED, microwave spectroscopy, high-resolution infrared and Raman spectroscopy and liquid-crystal NMR spectroscopy,[11] making this a perfect example for study using path-integral MD methods.

The method has also been applied to 1,3,5-trichlorotriazine, $C_3N_3Cl_3$, which was chosen because of its relative rigidity and the absence of hydrogen atoms. Its small size also means that DFT-PIMD simulations can be performed. This compound has a number of synthetic uses, including in the preparation of acyl azides and the pesticide atriazine.[12] $C_3N_3Cl_3$ has been the subject of a number of structural studies[13,14] in the solid state because of the anisotropic nature of the Cl···N interactions, which have proved difficult to model correctly without complex repulsive potentials.[15]

Experimental Section

Geometry Optimizations. The paper reporting the GED structures of $Si_8O_{12}H_8$ and $Si_8O_{12}Me_8$[8] in terms of their chemical interest contains some information about standard geometry optimizations performed for these compounds. Briefly, it was found that the bond lengths and angles calculated at the MP2/6-311++G(3df,3pd) level agreed best with the GED-determined structures. Without the extra polarization functions the bonded distances to Si were overestimated.

For $C_3N_3Cl_3$, calculations were carried out with the Gaussian 03 suite of programs,[16] mainly using resources provided by the UK National Service for Computational Chemistry Software.[17] Additionally, use was made of the resources of the EaStCHEM Research Computing Facility.[18] Calculations were initially performed at a low level, using the spin-restricted Hartree−Fock (RHF) method and the 3-21G(d)[19] basis set developed by Pople. A geometry optimization was carried out together with a frequency calculation, to ensure that the optimized structure corresponded to a minimum on the PES. Further calculations were conducted using larger Pople-style basis sets, namely 6-31G(d)[20] and 6-311+G(d).[21] The electron correlation energy was included using second-order Møller−Plesset perturbation theory (MP2)[22] and density functional theory (DFT) calculations were also carried out using the hybrid functional B3LYP.[23]

The geometries of $Si_8O_{12}H_8$, $Si_8O_{12}Me_8$ and $C_3N_3X_3$ (X = H, Cl) are shown in Figure 1 along with the atom numbering schemes used throughout.

Plane-Wave DFT Molecular Dynamics (DFT-MD). Descriptions of the DFT-MD simulations performed for the two silsesquioxanes are given in the paper reporting the GED structures of $Si_8O_{12}H_8$ and $Si_8O_{12}Me_8$.[8] The classical DFT-MD simulations of $C_3N_3H_3$ and $C_3N_3Cl_3$ were carried out in a similar fashion. The Car−Parrinello molecular dynamics (CPMD) code[24] was used running on the BlueGene/L computer at the Edinburgh Parallel Computing Centre.[25] Simulating an isolated gas molecule using a periodic code such as CPMD requires the use of a supercell to prevent interactions between that molecule and its periodic images. A cubic supercell of 14 Å was used together with a Tuckerman−Poisson solver[26] to ensure negligible interactions between periodic images. A plane-wave cutoff energy of 1250 eV was used for both compounds, with an increase in this value leading to changes in the atomic forces of less than 1 meV $Å^{-1}$. The PBE exchange-correlation functional[27] was used along with Troullier−Martins norm-conserving pseudopotentials.[28] The optimized geometry was calculated at this level of theory and used as the starting point for an NVT simulation. The simulation temperature was chosen to match the average temperature of the relevant GED experiment (387 and 398 K, respectively, for $C_3N_3H_3$ and $C_3N_3Cl_3$) and was controlled using a so-called "massive chain"[29] of Nosé−Hoover thermostats.[30] A time step of 121 as was used

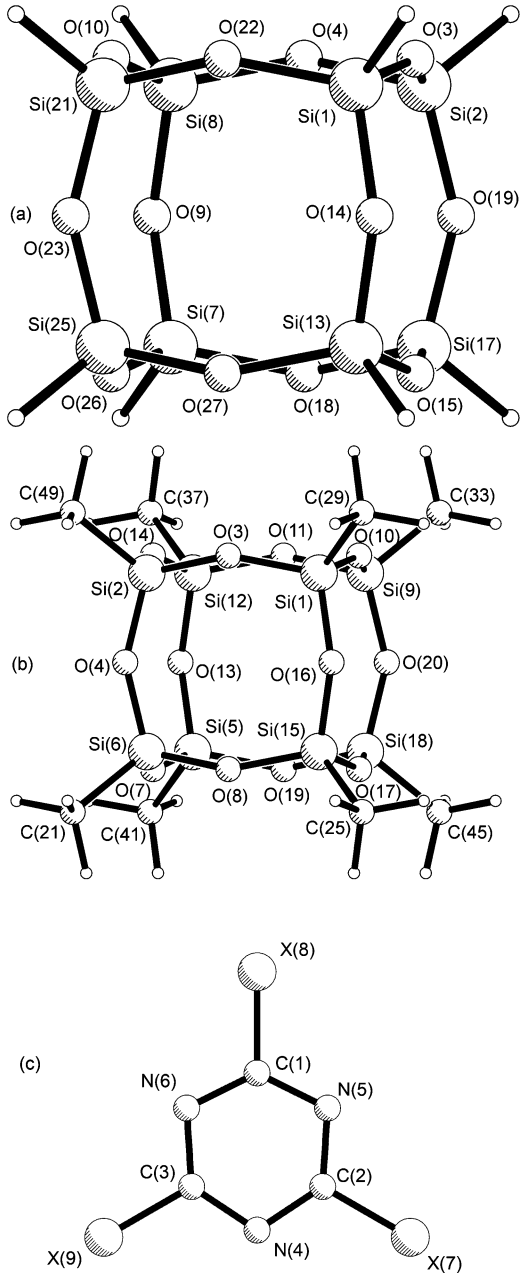

Figure 1. Molecular geometries of (a) $Si_8O_{12}H_8$, (b) $Si_8O_{12}Me_8$, and (c) $C_3N_3X_3$ (X = H, Cl) including atom numbering. Numbering of hydrogen atoms in (a) and (b) has been omitted for clarity, although coordinates for all atoms are included in Supporting Information (Tables S1 and S2) and can be used to identify these atoms.

for both simulations, with data collected every five steps for a total simulation length of 55 ps for $C_3N_3H_3$ and 41 ps for $C_3N_3Cl_3$.

Path-integral MD simulations of both compounds were carried out using the CPMD program using the same cutoff, cell size, time step, and thermostating as the classical simulations. The standard normal mode transformation approach[9] was used to propagate the equations of motions of the PI beads. For $C_3N_3H_3$ simulations using 12 and 32 beads were performed for 20 and 8 ps, respectively. The shorter simulation times are justified by the fact that all of the PI beads are equivalent to one another and therefore we are collecting 12 and 32 times the number of data points as compared to a classical simulation. A single PIMD simulation of $C_3N_3Cl_3$ was performed using 16 beads with data collected for 20 ps.

Empirical-Potential Molecular Dynamics (EP-MD). Empirical-potential molecular dynamics (EP-MD) simulations should run much quicker than DFT-MD simulations. It was therefore deemed worthwhile to run such simulations using a set of empirical potentials for $Si_8O_{12}H_8$ and $Si_8O_{12}Me_8$. These simulations were performed using the DL_POLY software[31] and the hybrid-COMPASS (HC) force field[32] with resources provided by the EaStCHEM Research Computing Facility.[18] The equilibrium structures of both silsesquioxane molecules were determined by cooling the molecule from room temperature to 0 K. Unfortunately, during the optimization the methyl groups of $Si_8O_{12}Me_8$ rotated by 60° with respect to the conformation determined by the MP2 and DFT calculations (i.e., that shown in Figure 1b). As the force field was apparently unable to predict the same conformation as the ab initio methods, it was decided only to perform an EP-MD simulation for $Si_8O_{12}H_8$. This simulation was run starting from the equilibrium geometry using the canonical (NVT) ensemble for 30 ps. A single Nosé−Hoover thermostat[30] maintained the same temperature as used in the corresponding DFT-MD simulation.

Velocity Autocorrelation Functions. Simulated vibrational spectra are often compared to experimental ones as a means of gauging the accuracy of computational methods. Here the vibrational spectra for $Si_8O_{12}H_8$ were calculated for both the DFT-MD and EP-MD simulations by Fourier transformation of the velocity autocorrelation functions[33] (VAF). Blackman windowing functions[34] were used to reduce errors resulting from the truncation of the data sets.

Analysis of MD Trajectories. ***Amplitudes of Vibration and Distance Corrections.*** Regardless of which MD method is used to obtain the simulated trajectory, the technique of obtaining the relevant data remains the same. A distance, r_a, obtained directly from a GED experiment, represents the inverse of the vibrationally averaged inverse of the distance between atoms i and j. This can be calculated directly from an MD simulation using

$$r_{a,ij} = \left(\frac{1}{N} \sum_{k=1}^{N} (r_{ij,k})^{-1} \right)^{-1} \quad (1)$$

where N is the total number of steps and $r_{ij,k}$ is the separation of the ith and jth atoms at the kth step in the trajectory. The distance correction used in a GED refinement is simply $(r_a - r_e)$, derived for each atom pair as described above. In all analyses of MD trajectories the first few picoseconds of data have been ignored to allow the system to achieve equilibration in terms of kinetic and potential energy.

It should be noted that the equations of motion of a classical harmonic oscillator lead to a probability distribution that is the "inverse" of the quantum mechanical result. However, molecular dynamics simulations are based on the assumption that the time-average result of the simulation corresponds to an ensemble average. The simulation is based on classical mechanics insofar as the evolution of the simulation treats the particles classically, but if we insert the classical harmonic potential $V(r) = kx^2$ into the Boltzmann relationship (eq 8 below), we obtain a Gaussian probability distribution just as in the quantum case. It is perhaps better to say that MD simulations are based on classical statistical mechanics rather than on classical mechanics.

Root-mean-square (rms) amplitudes of vibration (u) can be extracted from a simulation by obtaining the square of the difference between the instantaneous distance between atoms i and j at each time step and the average $i-j$ distance throughout

the entire simulation. This is then averaged over the number of steps, then over symmetrically equivalent atom pairs and finally the square root is taken as shown

$$u_{ij} = \left(\frac{1}{N_p N_s} \sum_{p=1}^{N_p} \sum_{k=1}^{N_s} (r_{ij,k,p} - \langle r_{ij,p} \rangle)^2 \right)^{1/2} \quad (2)$$

where N_s and N_p are the number of steps and number of equivalent pairs, respectively, and

$$\langle r_{ij,p} \rangle = \frac{\sum_{1}^{N} r_{ij}}{N_s} \quad (3)$$

The uncertainty in the time-averaged bond length, $\Delta r_{a,ij}$, obtained from an MD simulation can be estimated from the central limit theorem,[33] and is given by

$$\Delta r_{a,ij} = \frac{u_{ij}}{\sqrt{N_s}} \quad (4)$$

As there is no uncertainty in the equilibrium geometry, $\Delta r_{a,ij}$ is also the uncertainty in the $r_a - r_e$ corrections that are applied to the experimental structure. The uncertainty in the amplitude of vibration is given by a similar equation,

$$\Delta u_{ij} = \sqrt{\frac{2}{N_s - 1}} u_{ij} \quad (5)$$

The analysis of the PIMD simulations was performed using the above equations and considering each replica of the system in turn so that for a P-bead simulation P times as many distances are used for the calculations in eqs 2 and 3.

Morse Constants. The formula conventionally used to calculate the molecular-scattering intensity for a GED least-squares refinement[35] is

$$I_{mol}(s) = c \sum_{i=1}^{K} n_{ij} \frac{g_{ij}(s)}{r_{a,ij}} \exp\left(-\frac{1}{2} u_{ij}^2 s^2 \right) \sin[s(r_{a,ij} - \kappa_{ij} s^2)] \quad (6)$$

where K is the number of nonequivalent internuclear distances, c is the scale constant, n_{ij} is the multiplicity of the ijth pair of atoms, κ_{ij} is an asymmetry constant and $g_{ij}(s)$ is the scattering function, $|f_i(s)||f_j(s)| \times \cos[\eta_i(s) - \eta_j(s)]$, where $f_i(s)$ is the scattering factor for atom i and $\eta_i(s)$ is the phase of the ith atom. The asymmetry constant, κ, can, to a good approximation, be related to the constant a present in the Morse anharmonic potential[35]

$$\kappa = \frac{a u^4}{6} \quad (7)$$

For small molecules such as lanthanide trihalides, the asymmetry constants for bonded distances may be determined experimentally as independent parameters in the least-squares refinement procedure.[36] For larger molecules such determination becomes very unreliable, and in all cases asymmetry constants are usually assumed to be zero for nonbonded atom pairs. None of the existing approaches for determining amplitudes of vibration and distance corrections[3−5] allow asymmetry constants to be evaluated from force-field calculations.

It is, however, possible to determine the Morse constants and, therefore, the asymmetry constants from the trajectory of an MD simulation. The instantaneous interatomic distances adopted by an atom pair can be easily binned during the course of the simulation to determine a histogram of atomic distances. Normalization of this histogram produces a probability density function, $P(r)$, for each pair of atoms. The Boltzmann equation relates this function to the effective interatomic potential $V(r)$ such that

$$P(r) = \frac{1}{Z} e^{-V(r)/k_B T} \quad (8)$$

where k_B is the Boltzmann constant and Z is the partition function. The potential can be obtained from

$$V(r) = -k_B T \{ \ln[P(r)] - \ln[P(r_e)] \} \quad (9)$$

The subtraction of $\ln[P(r_e)]$ gives $V(r_e) = 0$ and eliminates the partition function, Z, from eq 9. A Morse potential function is given by

$$V(r) = D_e (1 - e^{-a(r - r_e)})^2 + V(r_e) \quad (10)$$

where D_e represents the dissociation constant. Regression methods can then be used to fit the Morse potential to the tabulated potential obtained using eq 9, yielding a value for the Morse constant that can then be used in the GED refinement.

Harmonic and Anharmonic Force-Field Methods. Using Gaussian 03,[16] harmonic force fields were computed at the B3LYP level using 6-311++G(d,p) basis sets on all atoms for $Si_8O_{12}H_8$ and $Si_8O_{12}Me_8$. These were then used to generate rms amplitudes of vibration and distance corrections with the SHRINK program.[4,5] The amplitudes of vibration and distance corrections were generated for use in the GED refinement process and for comparison with those generated by the new MD approach. Third derivatives of the energy were also calculated at this level to apply to the distance corrections the cubic anharmonic contributions for which SHRINK also makes provision.

For $C_3N_3Cl_3$, harmonic and anharmonic force fields were calculated at the B3LYP/6-311+G(d) level. These were used with SHRINK to produce rms amplitudes of vibration and distance corrections that would allow the r_{h1} and $r_{a3,1}$ structures to be determined. The $r_{a3,1}$ nomenclature is discussed in detail in ref 6.

Gas Electron Diffraction. The gas electron diffraction (GED) experiments for the silsesquioxanes are not the primary focus of this paper, and details are available elsewhere.[8] In any case they follow very closely the procedure described here for $C_3N_3Cl_3$.

Data for $C_3N_3Cl_3$ were collected using the Edinburgh GED apparatus[37] with an accelerating voltage of 40 kV (equivalent to an electron wavelength of approximately 6.0 pm). Experiments were performed at two different nozzle-to-film distances to maximize the range of scattering data available. The scattering intensities were recorded on Kodak Electron Image films, and

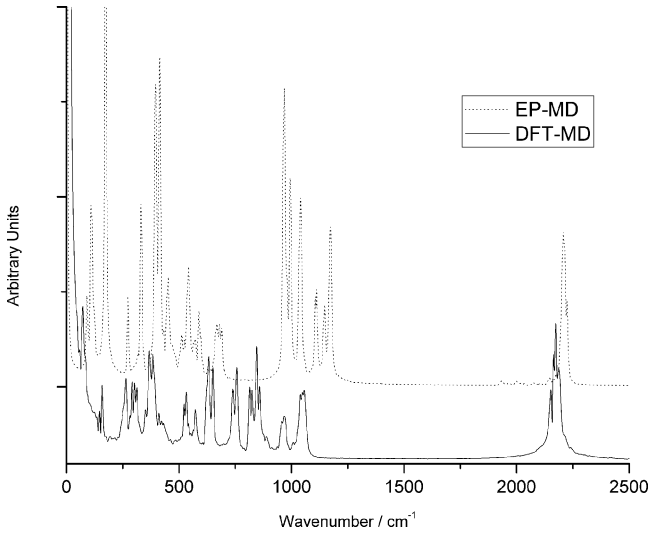

Figure 2. Vibrational spectra for $Si_8O_{12}H_8$ determined from the EP-MD and DFT-MD simulations.

nozzle-to-film distances are given in Table S3 (Supporting Information). The nozzle and sample temperatures were approximately 408 and 398 K for both nozzle-to-film distances. (Normally an increased temperature is required for the shorter nozzle-to-film distance, but in this case a more intense electron beam allowed the temperatures to be the same.) The camera distances were calculated using diffraction patterns of benzene recorded immediately after each of the sample runs. The scattering intensities were measured using an Epson Expression 1680 Pro flatbed scanner and converted to mean optical densities using a method described elsewhere.[38] The data were then reduced and analyzed using the ed@ed v2.4 least-squares refinement program[39] employing the scattering factors of Ross et al.[40] The weighting points for the off-diagonal weight matrix, correlation parameters and scale factors are shown in Table S3 (Supporting Information).

Results and Discussion

$Si_8O_{12}H_8$. ***Vibrational Analysis.*** The vibrational spectrum of $Si_8O_{12}H_8$ determined using the VAF is shown for both the DFT-MD and EP-MD simulations in Figure 2. The peak positions and other theoretical and experimental results[41] are listed in Table S4 (Supporting Information). The agreement between the experimental and theoretical results is reasonable, particularly for the DFT-MD results. We can therefore expect the MD simulations to provide a good representation of thermal motion in the silsesquioxanes. The DFT-MD and EP-MD frequencies are typically smaller than those obtained from the B3LYP harmonic frequency calculation. This softening of the vibrations is expected as both MD simulations allow for anharmonic motion. The DFT-MD Si−H stretching frequencies will be further reduced by the drag of the fictitious electron mass used in Car−Parrinello dynamics.[42]

rms Amplitudes of Vibration, Distance Corrections, and Asymmetry Constants. The rms amplitudes of vibration determined for $Si_8O_{12}H_8$ using the traditional rectilinear (h0) and curvilinear (h1) approaches as well as those obtained from the MD simulations are presented in Table 1. The amplitudes determined by the MD methods are typically smaller than those from the force-field methods. This discrepancy is greatest for the Si−H bonded distance (u_1), for which the DFT-MD simulation gives an amplitude that is only 43% of the u_{h0}/u_{h1} value. The EP-MD simulation gives a slightly larger value of 4.53 pm, but this is still only 52% of the value calculated using traditional methods. This is at first sight unexpected as the vibrational frequencies obtained from the harmonic force field (which was used to calculate the u_{h0} and u_{h1} values) and from the MD simulations are in much better agreement than the differences in amplitudes suggest. In general, the agreement is better for longer nonbonded distances and for those involving heavier atoms. For example, the discrepancy for O(3)···O(4) of only around 20% suggests that the discrepancies arise because of the classical modeling of molecular motion.

The amplitudes of vibration calculated by the traditional methods use a quantum-mechanical regime, whereas both types of MD simulation move the atoms classically. (Even though the DFT method calculates the forces quantum mechanically the atomic trajectories are still calculated using Newton's equations of motion.) Quantum mechanically, the rms amplitudes of vibration would be larger as the wave function can spread into classically forbidden areas. The Debye temperature gives an indication of whether a classical approach is valid at a given temperature. The relationship is

$$\theta_D = \frac{h\nu_m}{k_B} \tag{11}$$

where θ_D is the Debye temperature, h is Planck's constant, ν_m is the Debye frequency, and k_B is the Boltzmann constant. From this relationship it can be determined that, at a temperature of 400 K, frequencies of vibration above about 280 cm^{-1} should be treated with a quantum-mechanical approach. The vast majority of the vibrational contributions to the rms amplitudes of vibration will therefore be underestimated if a classical approach is taken. However, it is difficult to quantify the effects of neglecting quantum dynamics, particularly for nonbonded distances, where many low-frequency vibrations will dominate the motions of atoms.

A brief note is required to clarify the notation used for the distance corrections. The distance corrections, "k", determined by SHRINK using harmonic force fields represent the corrections for motions perpendicular to the vector linking the two atoms in question. The full correction also includes a component (u^2/r) to account for the distance correction along the vector. The distance corrections quoted here ($r_a - r_{hn}$) for comparison with those from the anharmonic approach using SHRINK and from the MD approaches are therefore equal to $k - u^2/r_a$. Both the a3,1 and MD approaches directly yield corrections that convert from r_a to $r_{a3,1}$ or $r_{e,MD}$ and are quoted as $r_a - r_x$.

The distance corrections obtained from the h0 and h1 approaches have vastly differing values, illustrating the limitations of a simplistic rectilinear approximation of vibrational motion. The inclusion of cubic anharmonicity shifts the distance corrections for the bonded distances from negative values in the h1 approach to positive values in the a3,1 approach. The a3,1 distance corrections are typically larger than those from the MD simulations for the shorter interatomic distances in the molecule. This is expected, as any underestimation of the thermal motion will shorten distance corrections, especially if there is a significant degree of curvilinear motion. However, for most of the longer distances in the molecule, the DFT-MD method yields corrections larger than the cubic-force-field approach.

This is not the case for the EP-MD results, which are in reasonable agreement with the a3,1 corrections despite the rms amplitudes of vibration being underestimated by this method

TABLE 1: Calculated rms Amplitudes of Vibration (u) and Distance Corrections ($r_a - r_x$) and Morse Constants (a) for $Si_8O_{12}H_8$[a]

	rms amplitudes of vibration				distance corrections					Morse constants
atom pair	u_{h0}	u_{h1}	$u_{DFT\text{-}MD}$	$u_{EP\text{-}MD}$	$r_a - r_{h0}$	$r_a - r_{h1}$	$r_a - r_{a3,1}$	$r_a - r_{e,DFT\text{-}MD}$	$r_a - r_{e,EP\text{-}MD}$	$a_{DFT\text{-}MD}$
Si(1)−H(5)	8.6	8.6	3.7(1)	4.5(1)	1.7	−0.6	1.8	0.5(1)	0.6(1)	13.8
Si(1)−O(3)	4.5	4.7	2.9(1)	3.3(1)	1.9	−0.2	0.7	0.6(1)	0.3(1)	28.5
O(3)···H(5)	12.1	12.1	7.5(1)	8.2(1)	2.1	−0.6	1.9	1.1(1)	0.6(1)	6.1
O(3)···O(4)	8.4	9.2	7.2(1)	7.5(1)	2.6	−1.5	0.4	0.1(1)	−0.2(1)	0.7
Si(1)···Si(2)	9.1	9.8	6.4(1)	6.7(1)	−0.2	−3.3	−1.2	−0.9(1)	−0.5(1)	0.0
O(3)···O(10)	38.2	38.7	29.9(4)	21.0(3)	−6.4	−12.2	−4.7	−4.6(3)	−2.1(2)	0.0
Si(1)···O(4)	20.2	20.7	15.3(2)	12.7(2)	−3.0	−5.9	−2.1	−2.0(2)	−1.1(1)	0.0
Si(1)···H(6)	12.5	13.7	8.2(1)	9.0(1)	0.0	−4.8	−0.7	−1.0(1)	−0.6(1)	0.0
Si(1)···Si(8)	9.3	10.0	7.2(1)	8.3(1)	−0.2	−4.6	−1.6	−1.2(1)	−0.8(1)	0.0
O(3)···O(9)	24.9	25.6	16.5(2)	15.6(2)	−2.2	−9.2	−3.5	−3.3(2)	−1.9(2)	0.0
H(5)···H(6)	22.7	24.6	15.3(2)	16.0(2)	−1.3	−7.1	−1.2	−1.5(2)	−1.1(2)	0.0
O(3)···H(12)	20.9	21.9	16.2(2)	13.6(1)	−0.8	−7.2	−1.8	−2.1(2)	−1.2(1)	0.0
Si(1)···O(9)	19.0	19.5	12.9(2)	13.5(2)	−0.9	−7.3	−2.8	−2.5(1)	−1.5(1)	0.0
O(3)···O(26)	24.4	25.0	17.0(2)	16.0(2)	−1.7	−10.0	−3.8	−3.4(2)	−2.2(2)	0.0
Si(1)···Si(7)	9.0	9.3	6.1(1)	10.5(2)	−0.2	−5.6	−2.0	−1.5(1)	−1.1(1)	0.0
Si(1)···H(12)	14.5	15.5	9.8(1)	11.4(2)	−0.2	−6.6	−1.5	−1.6(1)	−1.1(1)	0.0
O(3)···H(11)	21.2	21.9	13.6(2)	14.5(2)	−0.5	−9.1	−2.5	−2.8(1)	−1.8(1)	0.0
H(5)···H(12)	19.2	21.0	13.1(2)	13.9(2)	−0.3	−8.4	−1.4	−2.0(1)	−1.4(1)	0.0
Si(1)···H(11)	12.3	12.7	7.2(1)	11.5(2)	0.1	−7.5	−1.8	−1.9(1)	−1.3(1)	0.0
H(5)···H(11)	14.8	15.4	8.7(1)	12.4(2)	0.1	−9.7	−1.7	−2.4(1)	−1.7(1)	0.0

[a] Distances and amplitudes are in pm, while Morse constants are in nm^{-1}. Values in parentheses are the standard deviations on the last digits. See Figure 1a for atom numbering.

as well. Both the a3,1 and EP-MD approaches are restricted in the degree of anharmonicity that they can represent. The DFT approach can allow for any degree of anharmonicity so long as the method accurately represents the thermal motion of the system.

When the corrections given in Table 1 are compared, all of the various methods show that the silsesquioxane cage contracts due to the effects of anharmonic thermal motion. The largest interatomic contraction is for O(3)···O(10), which features the largest amplitude motion. The complex motions of the cage may therefore provide a model for negative thermal expansion of zeolites that contain similar cage structures. In particular, it should be noted that for many cross-cage atom pairs the anharmonicity is negative. It is this negative anharmonicity that leads to shortening of these interatomic distances as the temperature rises.

The DFT-MD simulation only yields nonzero Morse constants for the two bonded distances and for the two shortest nonbonded distances. For bonded distances a Morse potential should provide a reasonable physical model but the nonbonded effective potentials are poorly described by a Morse curve. The effective potential will include the averaged effects of all of the complex dynamics involving both atoms in the distance pair. More complex potentials could be modeled properly using a more generic scattering equation such as that of McCaffrey et al.[43] We might expect shorter interatomic distances involving terminal atoms to feature some Morse character as the O(3)···H(5) distance does in this case.

Diatomic Morse constants have been tabulated by Kuchitsu et al.,[44] using experimental values published by Huber and Herzberg.[45] The tabulated Si−O value of 19.7 nm^{-1} is smaller than the value determined here (28.5 nm^{-1}), while there is better agreement between the tabulated Si−H value of 15.3 nm^{-1} and the MD value of 13.8 nm^{-1}. Discrepancies may arise in part from the neglect of quantum dynamics in the DFT-MD method. However, there is scant experimental information on Morse parameters in large molecules, so little more can be said at this time.

GED Refinement. The GED structure of $Si_8O_{12}H_8$ has recently been published.[8] As this work is already available, we will briefly recall that O_h symmetry was assumed, so only three geometric parameters, rSi−O, rSi−H, and ∠Si−O−Si, were required. The published structure was determined using distance corrections generated using the DFT-MD method, and starting values for amplitudes of vibration were determined using SHRINK with a force field calculated at the B3LYP/6-311++G(d,p) level. Here for the first time we present the results of the refinement using rms amplitudes of vibration and distance corrections obtained solely from the cubic force field using SHRINK (the so-called $r_{a3,1}$ refinement).

The important parameters from the $r_{a3,1}$ refinement were rSi−O = 161.37(3) pm, rSi−H = 145.2(8) pm, ∠Si−O−Si = 148.4(2)°, and R_G = 0.051 (R_D = 0.032). For comparison the published values (using DFT-MD distance corrections and SHRINK amplitudes of vibration) were rSi−O = 161.41(3) pm, rSi−H = 145.4(8) pm, ∠Si−O−Si = 147.9(2)°, and R_G = 0.051 (R_D = 0.032). It can be seen that these refinements yielded very similar results, which is not surprising considering that the distance corrections (shown in Table 1) from the two methods are very similar. As discussed earlier, the DFT-MD amplitudes of vibration were thought to be inaccurate and so were not used in any refinement.

$Si_8O_{12}Me_8$. *rms Amplitudes of Vibration, Distance Corrections and Asymmetry Constants.* Selected rms amplitudes of vibration and difference corrections determined for $Si_8O_{12}Me_8$ are presented in Table 2, while Table S5 (Supporting Information) lists all amplitudes of vibration and distance correction values. As the simulation for $Si_8O_{12}Me_8$ was performed at a substantially higher temperature than those for $Si_8O_{12}H_8$, we expect the neglect of quantum dynamics in the MD simulations to be less important, although still evident. In particular, the C−H bond has an amplitude of half of what would be expected, and this is mainly because the main contribution to the motion between the bonded C and H atoms is the stretching vibration, which has a very high frequency compared with all of the other vibrations in the molecule.

In general, the SHRINK amplitudes of vibration are substantially larger than those predicted by the DFT simulation. The corrections and vibrational amplitudes for $Si_8O_{12}Me_8$ are larger than those for corresponding distances in $Si_8O_{12}H_8$. We expect

TABLE 2: Selected Calculated rms Amplitudes of Vibration (u), Distance Corrections ($r_a - r_x$), and Morse Constants (a) for $Si_8O_{12}Me_8$[a]

atom pair	rms amplitudes of vibration		Distance corrections			Morse constants
	u_{h1}	u_{DFT-MD}	$r_a - r_{h1}$	$r_a - r_{a3,1}$	$r_a - r_{e,DFT-MD}$	a_{DFT-MD}
C(21)−H(22)	7.6	3.5(1)	−0.2	1.6	0.5(1)	18.6
Si(1)−O(3)	5.8	4.2(1)	−0.1	1.0	0.8(1)	22.4
O(3)···H(31)	26.7	24.9(2)	2.3	−6.2	1.9(2)	0.7
Si(1)···Si(2)	17.7	9.3(1)	−7.4	2.9	−1.5(1)	0.0
O(3)···O(8)	64.2	35.4(3)	−13.0	−16.4	−5.6(2)	0.0
O(3)···O(7)	47.5	25.7(2)	−16.5	−14.8	−4.4(2)	0.0
H(22)···H(44)	80.6	46.7(4)	−21.7	−13.0	−2.8(3)	−1.0
O(3)···O(19)	39.5	31.3(3)	−19.3	−10.3	0.3(2)	0.0
O(3)···H(23)	38.9	22.7(2)	−20.0	−10.6	0.3(2)	0.0
O(3)···C(41)	37.4	47.4(5)	−19.9	−7.0	9.3(3)	0.5
Si(1)···C(41)	15.0	10.5(1)	−17.9	−24.4	−3.1(1)	0.0

[a] Distances and amplitudes are in pm, while Morse constants are in nm^{-1}. Values in parentheses are the standard deviations on the last digits. See Figure 1b for atom numbering. For a complete list of values see Table S5 in the Supporting Information.

this increase as the Me groups emphasize the low-frequency vibrations of the Si_8O_{12} cage, which leads to larger amplitudes and more anharmonic motion. This can be seen for the O(3)···O(8) distance in $Si_8O_{12}Me_8$, which corresponds to the O(3)···O(10) distance in $Si_8O_{12}H_8$. In terms of the distance corrections computed for $Si_8O_{12}Me_8$, the values determined by the DFT simulation are substantially bigger than the h1 and a3,1 values. Again this is probably due to these methods underestimating the anharmonicity of the system.

Previous structural studies of $Si_8O_{12}H_8$ and $Si_8O_{12}Me_8$ in the crystalline phase have shown that the O atoms are flexible and that there are large-amplitude vibrations of O atoms transverse to the Si−O−Si linkers.[46,47] Such vibrations correspond to atoms moving along large curved trajectories and the Me groups present in $Si_8O_{12}Me_8$ should lead to amplitudes larger than were present in $Si_8O_{12}H_8$. The H atoms will also move along circular trajectories as the methyl groups rotate. The h1 method models such vibrations with a harmonic function, while the a3,1 method treats them using a cubic function. From these functions the amplitudes and corrections are determined. Neither method is particularly suited to describing the strongly curvilinear motion that is probably occurring here. The DFT method allows us to determine the distance corrections and amplitudes of vibration numerically without making any assumptions about the types of motion present.

The values yielded by the MD simulations for the Morse constants are particularly pleasing. For nonbonded atom pairs the values are very close to zero, while for the bonded pairs the values are, as expected, close to 20 nm^{-1}.

GED Refinement. The published structure[8] of $Si_8O_{12}Me_8$ was determined using distance corrections and amplitudes of vibrations derived from the DFT-MD simulations. The molecule was assumed to have O_h symmetry and the model, which is described in greater detail elsewhere,[8] consisted of five geometric parameters: rSi−O, rSi−C, rC−H, ∠Si−O−Si, and ∠Si−C−H. For comparison, another refinement was performed using rms amplitudes of vibration and distance corrections determined from SHRINK [B3LYP/6-31G(d) anharmonic force field]; this is reported here. Unlike for $Si_8O_{12}H_8$, where the results of the $r_{a3,1}$ and $r_{e,MD}$ refinements were almost identical, here the results of the $r_{a3,1}$ refinement are much worse: rSi−O = 163.36(14) pm, rSi−C = 184.7(6) pm, rC−H = 110.0(9) pm, ∠Si−O−Si = 150.1(4)°, ∠Si−C−H = 111.8(9)°, and R_G = 0.233 (R_D = 0.204) compared to rSi−O = 161.74(5) pm, rSi−C = 182.9(3) pm, rC−H = 110.1(7) pm, ∠Si−O−Si = 148.9(2)°, ∠Si−C−H = 110.9(7)°, and R_G = 0.077 (R_D = 0.054). The final radial-distribution curve and the difference curves corresponding to both refinements are given in Figure 3. From the discussion in the previous section, where the very different amplitudes of vibration and distance corrections yielded by the different methods were highlighted, it is not surprising that a high-quality structure was not achievable from the $r_{a3,1}$ refinement. It is, however, pleasing that the structure could be determined when values obtained from the DFT-MD simulations were used.

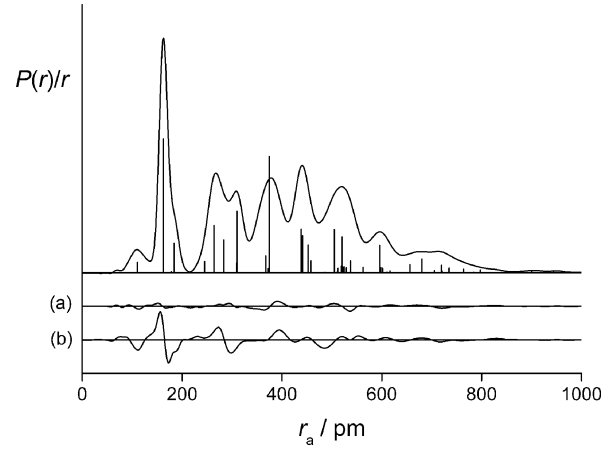

Figure 3. Experimental and theoretical-minus-experimental radial-distribution curves for $Si_8O_{12}Me_8$ from (a) the $r_{e,MD}$ refinement and (b) the $r_{a3,1}$ refinement. Before Fourier inversion the data were multiplied by $s\cdot\exp(-0.00002s^2)/(Z_O - f_O)(Z_{Si} - f_{Si})$.

PIMD Simulations of $C_3N_3H_3$. To illustrate how path-integral MD simulations can be used to overcome the deficiencies relating to the neglect of quantum dynamics encountered with the classical MD simulations (both EP and DFT), a series of PIMD simulations was performed for $C_3N_3H_3$ using 1, 12, and 32 beads. The resulting amplitudes of vibration, distance corrections and Morse constants are given in Table 3.

The classical simulation (i.e., where only one bead is used) gives a small value for the C−H amplitude similar to that found for the C−H bond in $Si_8O_{12}Me_8$. The PIMD simulations give larger amplitudes in all cases, leading to improved agreement with the experimental values. Although there are still discrepancies between the PIMD and experimental values, this is very likely due to the large uncertainties in the experimental values.

The distance corrections vary significantly between the classical and quantum simulations, particularly for the distances involving H atoms. In the case of the silsesquioxanes the large-amplitude, low-frequency modes should minimize the effect of quantum dynamics on the longer distance corrections. Encour-

TABLE 3: PIMD-Calculated rms Amplitudes of Vibration (u), Distance Corrections ($r_a - r_e$), and Morse Constants (a), for $C_3N_3H_3$ for Various Numbers of Beads, P, Together with Experimental rms Amplitudes of Vibration[a]

	$P = 1$			$P = 12$			$P = 32$			exp[b]
atom pair	u	$r_a - r_e$	a	u	$r_a - r_e$	a	u	$r_a - r_e$	a	u
C(1)−N(5)	3.4(1)	0.4	22.3	4.6(1)	0.7	17.2	4.7(1)	0.8	13.1	5.1(2)
C(1)−H(8)	3.3(1)	0.5	23.2	7.7(1)	1.6	10.1	7.8(1)	1.8	10.7	5.3(11)
C(1)···C(2)	4.1(1)	0.3	4.5	5.2(1)	0.8	6.6	5.2(1)	0.9	5.5	6.1(5)
N(4)···N(5)	4.5(1)	0.4	9.8	5.5(1)	0.8	4.8	5.6(1)	0.9	7.6	6.2(4)
N(4)···H(7)	5.9(1)	0.5	1.9	9.7(1)	1.5	2.7	9.9(1)	1.7	3.9	12.4(12)
C(1)···N(4)	5.2(1)	0.2	2.1	6.0(1)	0.8	2.5	6.2(1)	0.9	4.8	6.5(4)
C(1)···H(7)	5.6(1)	0.1	2.8	9.3(1)	1.5	4.1	9.4(1)	1.7	4.9	13.1(16)
N(4)···H(8)	6.2(1)	−0.3	0.3	9.4(1)	1.3	3.6	9.6(1)	1.5	3.6	12.0(29)
H(7)···H(8)	7.6(1)	−0.2	0.0	12.7(1)	1.9	2.4	12.9(1)	2.2	2.1	12.6(fixed)[c]

[a] Distances and amplitudes are in pm, while Morse constants are in nm^{-1}. Values in parentheses are the standard deviations on the last digits. See Figure 1c for atom numbering. [b] Values from the combined GED/IR/Raman/MW/LCNMR refinement from ref 11. [c] Fixed at the value determined by an experimental force field.

TABLE 4: Calculated and Experimental rms Amplitudes of Vibration (u), Distance Corrections ($r_a - r_x$), and Morse Constants for $C_3N_3Cl_3$[a]

	rms amplitudes of vibration			distance corrections			Morse constants	
atom pair	u_{h1}	$u_{DFT\text{-}PIMD}$	u_{GED}	$r_a - r_{h1}$	$r_a - r_{a3,1}$	r_a-$r_{e,DFT\text{-}PIMD}$	SHRINK[b]	MD
C(1)−N(5)	4.5	4.6(1)	4.7(1)	−0.1	0.6	0.6	22.7	21.7
C(1)−Cl(8)	4.8	5.2(1)	4.7(1)	0.0	0.8	0.9	18.3	21.5
C(1)···C(2)	5.2	5.3(1)	5.4 [tied to N(4)N(5)]	−0.6	0.6	0.7	0.0	0.3
N(4)···N(5)	5.3	5.5(1)	5.7(3)	−0.3	0.8	0.8	0.0	10.3
N(4)···Cl(7)	6.2	6.6(1)	6.7(1)	−0.2	1.0	1.1	0.0	9.5
C(1)···N(4)	5.9	6.2(1)	6.3 [tied to N(4)Cl(7)]	−0.7	0.7	0.7	0.0	2.1
C(1)···Cl(7)	6.2	6.6(1)	7.2(1)	−1.3	0.8	0.8	0.0	2.8
N(4)···Cl(8)	6.3	6.8(1)	7.7(2)	−1.6	0.7	0.6	0.0	1.3
Cl(7)···Cl(8)	8.4	8.5(1)	10.0(1)	−2.0	0.8	0.8	0.0	0.0

[a] Distances and amplitudes are in pm, Morse parameters are in nm^{-1}. Values in parentheses are the standard deviations on the last digits. See Figure 1c for atom numbering. [b] Tabulated values given in the SHRINK output, which are taken from ref 44. For nonbonded atom pairs values were set to zero.

agingly, the rms amplitudes and corrections from the 12- and 32-bead simulations for $C_3N_3H_3$ are within their respective uncertainties, suggesting that a modest number of beads is sufficient to obtain a suitable estimate of the amplitudes and corrections. The classical DFT-MD Morse constants for the bonded distances are in reasonable agreement with those tabulated by Kuchitsu et al.,[44] with the nonbonded values generally being much smaller than the bonded ones. However, the PIMD simulations give very different Morse constants when compared to the classical simulation and, unlike the amplitudes and distance corrections, these do not converge upon going from 12 to 32 beads. This probably reflects the greater uncertainties of these terms relative to those for amplitudes of vibration and distance corrections, and more precise values would be given by longer MD runs. While the analysis by averaging over replicas determines suitable amplitudes and corrections, the classical simulation clearly gives more reasonable Morse parameters. Analysis of the PIMD simulation by considering the centroid trajectory (averaging the P copies of each atom to obtain its centroid) produced poor amplitudes as well as poor Morse constants. The source of these discrepancies will be the focus of further work in developing this method.

$C_3N_3Cl_3$. rms Amplitudes of Vibration, Distance Corrections and Morse Constants. To provide a final check of the new methodology, we also studied a molecule that has no hydrogen atoms, and which has a relatively rigid structure. rms amplitudes of vibration were calculated for $C_3N_3Cl_3$ using SHRINK and also using the DFT-MD simulations. The same starting values for the amplitudes of vibration were used in the r_{h1} and $r_{a3,1}$ refinements; these were determined from a force field calculated at the B3LYP/6-31G(d) level. The amplitudes and distance corrections were calculated from the 16-bead DFT-PIMD simulation, while Morse constants were determined from the classical DFT-MD simulation because, as was the case for $C_3N_3H_3$, the PIMD simulations gave unacceptably small Morse constants for bonded atom pairs. Table 4 lists all atom pairs in $C_3N_3Cl_3$ and shows the various rms amplitudes of vibration, distance corrections, and Morse constants.

The amplitudes of vibration determined from the PIMD simulation are in excellent agreement with the cubic-force-field values and in the majority of cases with the experimental values. The agreement between the distance corrections is also extremely good. The relatively rigid structure of $C_3N_3Cl_3$ should lead to motions that will be well approximated by the cubic-force-field approach. The close agreement between the MD simulations and the ab initio results is a strong validation of the MD method.

The values of the Morse constants for the rC−N and rC−C bonded distances obtained from the MD simulations for $C_3N_3Cl_3$ are in the range of 21−22 nm^{-1}, which is in excellent agreement with the tabulated data for these distances available in the literature.[44] With the exceptions of N(4)···N(5) and N(4)···Cl(7) the values obtained for the nonbonded pairs of atoms are close to zero.

GED Refinement. The refinement of $C_3N_3Cl_3$ was performed using a D_{3h}-symmetric model comprising three parameters, rC−Cl, rC−N, and ∠N−C−N. Three separate refinements were performed, namely, r_{h1}, $r_{a3,1}$, and $r_{e,DFT\text{-}PIMD}$. For each refinement the three independent geometric parameters were refined by least-squares, as were seven amplitudes or groups of amplitudes of vibration. Table 5 gives the final parameter values from the refinements, highlighting the similarities, especially when values

TABLE 5: Calculated (r_e) and Final Parameters from the GED Refinements of $C_3N_3Cl_3$[a]

independent parameter		r_{h1}	$r_{a3,1}$	$r_{e,DFT-PIMD}$	r_e[b]
p_1	rC−Cl	171.16(9)	170.45(9)	170.24(9)	171.2
p_2	rC−N	132.87(6)	132.14(6)	132.14(6)	133.4
p_3	∠N−C−N	127.01(9)	127.13(10)	127.04(9)	126.9

[a] Distances are in pm, angles are in degrees. [b] Optimized geometry from an MP2/6-311+G(d) calculation. Coordinates and total energy are given in Table S9 of the Supporting Information.

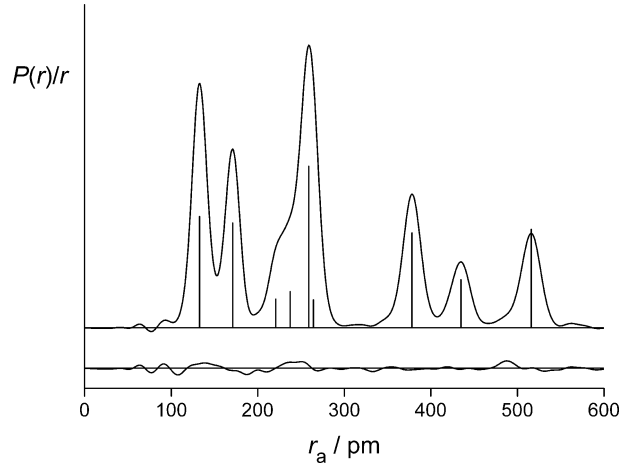

Figure 4. Experimental and theoretical-minus-experimental radial-distribution curves for $C_3N_3Cl_3$. Before Fourier inversion the data were multiplied by $s \cdot \exp(-0.00002s^2)/(Z_C - f_C)(Z_N - f_N)$.

from the $r_{a3,1}$ and $r_{e,DFT-PIMD}$ refinements are compared. Table S6 (Supporting Information) lists the refined amplitudes of vibration from the $r_{e,DFT-PIMD}$ refinement. The success of the $r_{e,DFT-PIMD}$ refinement can be assessed numerically using the final R factor, which was $R_G = 0.077$ ($R_D = 0.058$), and visually using the goodness of fit of the radial-distribution and difference curves as seen in Figure 4, and the molecular-scattering intensity curves (Figure S1 (Supporting Information)). The R_G values for the r_{h1} and $r_{a3,1}$ refinements were 0.079 and 0.081, respectively. The least-squares correlation matrix for the $r_{e,DFT-PIMD}$ refinement is given in Table S7 (Supporting Information) and coordinates for the final GED structure are in Table S8 (Supporting Information). A final test was performed by replacing the Morse constants used in the $r_{e,DFT-PIMD}$ refinement with those used in the r_{h1} and $r_{a3,1}$ refinements [namely, 22.7 nm^{-1} for C(1)−N(5), 18.3 nm^{-1} for C(1)−Cl(8), and 0.0 nm^{-1} for all nonbonded distances]. This made almost no difference to the refinement, with R_G improving by 0.001, thus demonstrating the relatively low importance that should be placed on the Morse constants used in GED refinements.

Conclusions

A new method of determining equilibrium structures of molecules, in principle of any complexity, in the gas phase has been developed, making use of rms amplitudes of vibrations, distance corrections and Morse constants derived from MD simulations. The method has been applied to the structure determinations of $Si_8O_{12}H_8$, $Si_8O_{12}Me_8$, and $C_3N_3Cl_3$. In two of the cases ($Si_8O_{12}H_8$ and $C_3N_3Cl_3$) the use of the new method yields results very close to those obtained using vibrational terms derived from calculated force fields, thereby demonstrating the reliability of the new method. The similarity of the refined $r_{a3,1}$ and $r_{e,DFT-PIMD}$ structures for $C_3N_3Cl_3$ is particularly impressive, and confirms the validity of the MD method for giving reliable vibrational correction terms. For $Si_8O_{12}Me_8$, where the presence of methyl groups on the outside of the silsesquioxane cage causes large-amplitude deformations of the cage itself that are not adequately modeled by calculated force fields, the MD simulations proved vital in determining the structure.

It is worth emphasizing that all methods—force field and MD—involve some degree of approximation. For many molecules harmonic, quadratic force fields will provide suitable estimates of vibrational motion. In other cases the introduction of anharmonic motion using cubic force fields will be necessary. However, there will still be cases where the inclusion of higher order terms would improve matters further; perhaps in the future we will be able routinely to calculate quartic force fields. Then there will be molecules whose vibrational motions are so anharmonic and which take the atoms into areas of space so far removed from their equilibrium positions that calculated force fields will always offer a poor representation. That is where this MD method will prove particularly useful.

We have identified a number of deficiencies in the basic MD method. Most notable was the inability of standard molecular dynamics simulations to incorporate the quantum dynamics of the nuclei. This resulted in underestimation of the amplitudes of vibration, particularly for the shorter distances that involve high-frequency vibrations, although fortunately the consequences for the distance corrections were not too severe. We have shown using simulations of $C_3N_3H_3$ that path-integral methods can overcome this deficiency, albeit at a significant extra cost in computational effort. The PIMD simulations do suffer from the fact that, at present, reliable Morse parameters cannot be extracted from the MD trajectories. The classical simulations give values that agree reasonably with literature values for bonded distances. Equally, there is little experimental evidence as to what magnitudes the values for nonbonded atom pairs should have and certainly no routine way of calculating either bonded or nonbonded values.

The types of MD simulation employed in the present work remain computationally intensive. However, developments in theory, linear scaling simulation codes,[48] and computational power should permit such simulations to be performed more routinely in the near future. Such advances should also allow for longer simulations, which will allow us to explore greater time scales and even more flexible molecules, which might feature increasingly complex intramolecular motions. Force-field and semiempirical methods may also be of use. The force field used to simulate $Si_8O_{12}H_8$ provided reasonable corrections and amplitudes, although it was unsuitable for $Si_8O_{12}Me_8$. Wherever force fields (e.g., the MM series[49] and AMBER[50]) or semiempirical methods are available that are highly optimized toward a particular class of compounds they should be expected to provide a reasonable description of the dynamics. We are now applying the new methodology to give equilibrium structures of several molecules that would otherwise be unobtainable.

Acknowledgment. We thank all those who provided computational resources, namely, the NSCCS, EaStCHEM RCF, and the EPCC. The electron diffraction work was funded by the EPSRC (EP/C513649). A.M.R. and P.D.M. enjoyed interesting and stimulating discussions with Prof. Paul Madden and Dr. J. Kay Dewhurst.

Supporting Information Available: Calculated coordinates for $Si_8O_{12}H_8$ and $Si_8O_{12}Me_8$, experimental details from the GED experiment and refinement of $C_3N_3Cl_3$, vibrational frequencies from experimental and theoretical methods for $Si_8O_{12}H_8$,

complete calculated rms amplitudes of vibration and distance corrections for $Si_8O_{12}Me_8$, refined and calculated amplitudes of vibration and calculated distance corrections for $C_3N_3Cl_3$, least-squares correlation matrix for the refinement of $C_3N_3Cl_3$. GED and calculated coordinates for $C_3N_3Cl_3$. This material is available free of charge via the Internet at http://pubs.acs.org.

References and Notes

(1) Jensen, P. *J. Mol. Spectrosc.* **1988**, *128*, 478. Jensen, P. *J. Chem. Soc., Faraday Trans. 2* **1988**, *84*, 1315.

(2) Bastiansen, O.; Traetteberg, M. *Acta Crystallogr.* **1960**, *13*, 1108. Breed, H.; Bastiansen, O.; Almenningen, A. *Acta Crystallogr.* **1960**, *13*, 1108. Morino, Y. *Acta Crystallogr.* **1960**, *13*, 1107.

(3) Hedberg, L.; Mills, I. M. *J. Mol. Spectrosc.* **1993**, *160*, 117. Hedberg, L.; Mills, I. M. *J. Mol. Spectrosc.* **2000**, *203*, 82.

(4) Sipachev, V. A. *THEOCHEM* **1985**, *22*, 143.

(5) Sipachev, V. A. In *Advances in Molecular Structure Research*; Hargittai, I. H. M., Ed.; JAI: Greenwich, 1999; Vol. 5, pp 323−371.

(6) McCaffrey, P. D.; Mawhorter, R. J.; Turner, A. R.; Brain, P. T.; Rankin, D. W. H. *J. Phys. Chem. A* **2007**, *111*, 6103.

(7) Reilly, A. M.; Wann, D. A.; Morrison, C. A.; Rankin, D. W. H. *Chem. Phys. Lett.* **2007**, *448*, 61.

(8) Wann, D. A.; Less, R. J.; Rataboul, F.; McCaffrey, P. D.; Reilly, A. M.; Robertson, H. E.; Lickiss, P. D.; Rankin, D. W. H. *Organometallics* **2008**, *27*, 4183.

(9) Tuckerman, M. E. *Path Integration via Molecular Dynamics*; John von Neumann Institute for Computing: Jülich, 2002; Vol. 10.

(10) Parrinello, M.; Rahman, A. *J. Chem. Phys.* **1984**, *80*, 860.

(11) Morrison, C. A.; Smart, B. A.; Rankin, D. W. H.; Robertson, H. E.; Pfeffer, M.; Bodenmüller, W.; Ruber, R.; Macht, B.; Ruoff, A.; Typke, V. *J. Phys. Chem. A* **1997**, *101*, 10029.

(12) Bandgar, B. P.; Pandit, S. S. *Tetrahedron Lett.* **2002**, *43*, 3413.

(13) Pascal, R. A., Jr.; Ho, D. M. *Tetrahedron Lett.* **1992**, *33*, 4707.

(14) Maginn, S. J.; Compton, R. G.; Harding, M. S.; Brennan, C. M.; Docherty, R. *Tetrahedron Lett.* **1993**, *34*, 4349.

(15) Mitchell, J. B. O.; Price, S. L.; Leslie, M.; Buttar, D.; Roberts, R. J. *J. Phys. Chem. A* **2001**, *105*, 9961.

(16) Frisch, M. J.; Trucks, G. W.; Schlegel, H. B.; Scuseria, G. E.; Robb, M. A.; Cheeseman, J. R.; Montgomery, J. A., Jr.; Vreven, T.; Kudin, K. N.; Burant, J. C.; Millam, J. M.; Iyengar, S. S.; Tomasi, J.; Barone, V.; Mennucci, B.; Cossi, M.; Scalmani, G.; Rega, N.; Petersson, G. A.; Nakatsuji, H.; Hada, M.; Ehara, M.; Toyota, K.; Fukuda, R.; Hasegawa, J.; Ishida, M.; Nakajima, T.; Honda, Y.; Kitao, O.; Nakai, H.; Klene, M.; Li, X.; Knox, J. E.; Hratchian, H. P.; Cross, J. B.; Adamo, C.; Jaramillo, J.; Gomperts, R.; Stratmann, R. E.; Yazyev, O.; Austin, A. J.; Cammi, R.; Pomelli, C.; Ochterski, J. W.; Ayala, P. Y.; Morokuma, K.; Voth, G. A.; Salvador, P.; Dannenberg, J. J.; Zakrzewski, V. G.; Dapprich, S.; Daniels, A. D.; Strain, M. C.; Farkas, O.; Malick, D. K.; Rabuck, A. D.; Raghavachari, K.; Foresman, J. B.; Ortiz, J. V.; Cui, Q.; Baboul, A. G.; Clifford, S.; Cioslowski, J.; Stefanov, B. B.; Liu, G.; Liashenko, A.; Piskorz, P.; Komaromi, I.; Martin, R. L.; Fox, D. J.; Keith, T.; Al-Laham, M. A.; Peng, C. Y.; Nanayakkara, A.; Challacombe, M.; Gill, P. M. W.; Johnson, B.; Chen, W.; Wong, M. W.; Gonzalez, C.; Pople, J. A. *Gaussian 03*, revision C.02; Gaussian, Inc.: Wallingford, CT, 2004.

(17) EPSRC National Service for Computational Chemistry Software. URL: http://www.nsccs.ac.uk.

(18) EaStCHEM Research Computing Facility (http://www.eastchem.ac.uk/rcf). This facility is partially supported by the eDIKT initiative (http://www.edikt.org).

(19) Binkley, J. S.; Pople, J. A.; Hehre, W. J. *J. Am. Chem. Soc.* **1980**, *102*, 939. Gordon, M. S.; Binkley, J. S.; Pople, J. A.; Pietro, W. J.; Hehre, W. J. *J. Am. Chem. Soc.* **1982**, *104*, 2797. Pietro, W. J.; Francl, M. M.; Hehre, W. J.; DeFrees, D. J.; Pople, J. A.; Binkley, J. S. *J. Am. Chem. Soc.* **1982**, *104*, 5039.

(20) Hehre, W. J.; Ditchfield, R.; Pople, J. A. *J. Chem. Phys.* **1972**, *56*, 2257. Hariharan, P. C.; Pople, J. A. *Theor. Chim. Acta* **1973**, *28*, 213. Gordon, M. S. *Chem. Phys. Lett.* **1980**, *76*, 163.

(21) Krishnan, R.; Binkley, J. S.; Seeger, R.; Pople, J. A. *J. Chem. Phys.* **1980**, *72*, 650. McLean, A. D.; Chandler, G. S. *J. Chem. Phys.* **1980**, *72*, 5639.

(22) Møller, C.; Plesset, M. S. *Phys. Rev.* **1934**, *46*, 618.

(23) Becke, A. D. *J. Chem. Phys.* **1993**, *98*, 5648. Lee, C.; Yang, W.; Parr, R. G. *Phys. Rev. B* **1988**, *37*, 785.

(24) CPMD, Copyright IBM Corp 1990−2006, Copyright MPI für Festkörperforschung Stuttgart 1997−2001.

(25) Edinburgh Parallel Computing Centre. URL: http://www.epcc.ed.ac.uk.

(26) Martyna, G. J.; Tuckerman, M. E. *J. Chem. Phys.* **1999**, *110*, 2810.

(27) Perdew, J. P.; Burke, K.; Ernzerhof, M. *Phys. Rev. Lett.* **1996**, *77*, 3865.

(28) Troullier, N.; Martins, J. L. *Phys. Rev. B: Condens. Matter Mater. Phys.* **1991**, *43*, 1993.

(29) Tobias, D. J.; Martyna, G. J.; Klein, M. L. *J. Phys. Chem.* **1993**, *97*, 12959.

(30) Nosé, S. *J. Chem. Phys.* **1984**, *81*, 511. Hoover, W. G. *Phys. Rev. A* **1985**, *31*, 1695.

(31) Smith, W. *Mol. Simul.* **2006**, *32*, 933. Smith, W.; Yong, C. W.; Rodger, P. M. *Mol. Simul.* **2002**, *28*, 385.

(32) Ionescu, T. C.; Qi, F.; McCabe, C.; Striolo, A.; Kieffer, J.; Cummings, P. T. *J. Phys. Chem. B* **2006**, *110*, 2502.

(33) Allen, M. P.; Tildesley, D. J. *Computer Simulation of Liquids*; Clarendon Press: Oxford, U.K., 1987.

(34) Harris, F. J. *Proc. IEEE* **1978**, *66*, 51.

(35) Hargittai, I. In *A Survey: The Gas-Phase Electron Diffraction Technique of Molecular Structure Determination in Stereochemical Applications of Gas-Phase Electron Diffraction, Part A*; Hargittai, I., Hargittai, M., Eds.; VCH Publishers: Weinheim, Germany, 1988.

(36) Zakharov, A. V.; Vogt, N.; Shlykov, S. A.; Giricheva, N. I.; Galanin, I. E.; Girichev, G. V.; Vogt., J. *J. Mol. Struct.* **2004**, *707*, 147.

(37) Huntley, C. M.; Laurenson, G. S.; Rankin, D. W. H. *J. Chem. Soc., Dalton Trans.* **1980**, 954.

(38) Fleischer, H.; Wann, D. A.; Hinchley, S. L.; Borisenko, K. B.; Lewis, J. R.; Mawhorter, R. J.; Robertson, H. E.; Rankin, D. W. H. *Dalton Trans.* **2005**, 3221.

(39) Hinchley, S. L.; Robertson, H. E.; Borisenko, K. B.; Turner, A. R.; Johnston, B. F.; Rankin, D. W. H.; Ahmadian, M.; Jones, J. N.; Cowley, A. H. *Dalton Trans.* **2004**, 2469.

(40) Ross, A. W.; Fink, M.; Hilderbrandt, R. In *International Tables for Crystallography*; Wilson, A. J. C., Ed.; Kluwer Academic Publishers: Dordrecht, The Netherlands, 1992; Vol. C, p 245.

(41) Marcolli, C.; Lainé, P.; Bühler, R.; Calzaferri, G.; Tomkinson, J. *J. Phys. Chem. B* **1997**, *101*, 1171.

(42) Tangney, P.; Scandolo, S. *J. Chem. Phys.* **2002**, *116*, 14.

(43) McCaffrey, P. D.; Dewhurst, J. K.; Rankin, D. W. H.; Mawhorter, R. J.; Sharma, S. *J. Chem. Phys.* **2008**, *128*, 204304.

(44) Kuchitsu, K.; Nakata, M.; Yamamoto, S. In *Joint Use of Electron Diffraction and High-Resolution Spectroscopy in Stereochemical Applications of Gas-Phase Electron Diffraction, Part A*; Hargittai, I., Hargittai, M., Eds.; VCH Publishers: Weinheim, Germany, 1988.

(45) Huber, K. P.; Herzberg, G. *Molecular Spectra and Molecular Structure, Part IV*; Van Nostrand Reinhold: New York, 1979.

(46) Törnroos, K. W. *Acta Crystallogr. C* **1994**, *50*, 1646.

(47) Auf der Heyde, T. P. E.; Bürgi, H.-B.; Bürgy, H.; Törnroos, K. W. *Chimia* **1991**, *45*, 38.

(48) VandeVondele, J.; Krack, M.; Mohamed, F.; Parrinello, M.; Chassaing, T.; Hutter, J. *Comput. Phys. Commun.* **2005**, *167*, 103.

(49) Allinger, N. L.; Chen, K. *J. Comput. Chem.* **1996**, *17*, 642.

(50) Cornell, W. D.; Cieplak, P.; Bayly, C. I.; Gould, I. R.; Merz, M. J.; Ferguson, D. M.; Spellmeyer, D. C.; Fox, T.; Caldwell, J. W.; Kollman, P. A. *J. Am. Chem. Soc.* **1995**, *117*, 5179.

JP904185G